AIMS Mathematics, 10(12): 30029–30052.
DOI:10.3934/math.20251320
Received: 19 October 2025
Revised: 03 December 2025
Accepted: 11 December 2025
Published: 22 December 2025

https://www.aimspress.com/journal/Math

Research article

Asymptotic behavior of soliton solutions of the Kairat-X model via the Hirota bilinear method: Painlevé integrability and machine learning analysis

Waseem Razzaq[1], **Asim Zafar**[1], **Naif Almusallam**[2,*] **and Fawaz Khaled Alarfaj**[2]

[1] Department of Mathematics, COMSATS University Islamabad, Vehari Campus, Pakistan
[2] Department of Management Information Systems, School of Business, King Faisal University, Al-Ahsa 31982, Saudi Arabia

* **Correspondence:** Email: nalmuslem@kfu.edu.sa.

Abstract: In this article, we investigated the integrability of the nonlinear dynamical Kairat-X model through Painlevé analysis, demonstrating that the equation satisfies the Painlevé property and is therefore integrable. We applied the bilinear Hirota method to derive several exact solutions, including breather wave, novel periodic wave, periodic cross-kink wave, kink-rogue wave interaction, and one-soliton and two-soliton solutions. A machine learning multi-layer-perceptron regressor algorithm was applied to represent the behavior of the actual, and to predict, the above solutions. Furthermore, we employed an asymptotic analysis on the gain solutions to expect the demonstration of the asymptotic behavior of these analytical solutions. The soliton solutions obtained were novel and exhibited improved reliability compared to previously reported results. These findings were further validated using symbolic computation software. A comparison with the existing literature revealed that the proposed solutions were more applicable and accurate. Several of the results were visualized using two-dimensional, three-dimensional, and contour surface plots.

Keywords: Kairat-X model; Painlevé analysis; Hirota bilinear method; soliton solutions; machine learning analysis; multi-layer-perceptron regressor; asymptotic analysis
Mathematics Subject Classification: 35A20, 35C08, 35Q55, 37K10

1. Introduction

Nonlinear evolution equations (NLEEs) play an essential role in describing a vast arrangement of physical phenomena that make an appearance in fluid dynamics, plasma physics, nonlinear optics, and quantum field theory. Because of its numerous uses in nonlinear research, soliton theory has become one of the most active areas in mathematical physics. Solitons, self-reinforcing solitary

waves, emerge in a multiple array of physical systems, from fluid dynamics and optical fibers to plasma physics and Bose-Einstein condensates. Soliton theory has been generally studied in several fields, including physics, mathematics, and engineering, and high-speed data transmission is made possible by optical solitons, which are light pulses that travel across optical fibers without dispersion. These wave structures, which conserve their shape and speed even after interactions, are foundational to understanding several nonlinear phenomena. Research on soliton theory is ongoing, with new findings and advancements occurring frequently. Quantum solitons, soliton-based computing, solitons in nonlinear lattices, topological solitons, and experimental realizations are some of the most modern and sophisticated areas of soliton theory. Researchers have made remarkable progress in understanding the behavior of solitons and their application in different systems. Creating new mathematical models that accurately depict how solitons behave in various systems and coming up with innovative methods for creating and modifying solitons are some of the major issues facing soliton theory. The underlying mathematical models that assist solitonic solutions are nonlinear partial differential equations (PDEs) that express integrability under particular conditions. The capacity of the Kairat-X equation, a generalized nonlinear partial differential equation, contributes as a rich mathematical model for studying such wave dynamics. This equation represents the cooperation between dispersion and nonlinearity and is known to exhibit a vast variety of nonlinear wave structures depending on the parameter scheme. The study of novel integrable and non-integrable NLEEs has received a lot of attention in an effort to examine their integrability characteristics and soliton solutions. The Kairat-X equation, introduced by Myrzakulov et al. [1],

$$u_{\mathrm{tt}} - 3(u_t u_x)_x + u_{\mathrm{xxxt}} = 0. \tag{1.1}$$

Many researchers such as, Xiao, Barak, and Hleili used the Riccati modified extended simple equation method in [2] on Kairat-II and Kairat-X equations, Wazwaz, A. M used Painlevé analysis to find the multiple soliton solutions [3], Myrzakulov and Umurzakhova used the novel auxilary equation method on the Kairat-II and Kairat-X equations to find traveling wave solutions [4], Seadawy and Alomari, F. A used the extended simplest equation method on fractional Kairat-X equation [5], Asim Zafar and M. Raheel used the expa function, modified simplest equation method, and generalized Kudryashov method on truncated M-fractional Kairat-X and Kairat-II equations [6], Mathanaranjan, T. used the Lie symmetries method on the Kairat-II-X equation [7], Al-Sawalha and Mukhtar used the Riccati-Bernoulli sub-ODE technique and the Bäcklund transformation on confirmable Kairat equations [8], Rafiq and Alsaud used the Hirota bilinear method and linear superposition principle (LSP) on Kairat-X equation [9], Qahiti and Alsafri used the generalized $(r + \frac{G'}{G})$ expension method and simple $(\frac{G'}{G})$ method on Kairat-X equation [10] to obtain exact solutions of the Kairat-X equation.

In this paper, two analytical techniques are used for the Kairat-X equation, namely Painlevé analysis, to confirm the integrability, and Hirota bilinear exact soliton solutions, respectively. Exact solutions are obtained only when an equation is integrable and only integrable equations yield full analytic solutions. That is why, in this article, we use the analytical technique Painlevé analysis to find the integrability of a nonlinear differential equation. Over the past decade, many researchers executed Painlevé tests on the following equations: the nonlinear generalized variable coefficient KdV-type equation [11], the third order nonlinear Schrödinger equation [12], the extended Korteweg-de Vries equation [13], the variable-coefficient generalized Calogero–Bogoyavlenskii–Schiff equation [14], the generalized KP equation [15], the coupled Higgs equation [16], the Sasa–Satsuma equation [17], the

Sawada-Kotera, Lax and Caudrey-Dodd-Gibbon equations [18], the (3+1)-dimensional Boussinesq-type equation [19], the pseudo-parabolic type equations [20], and the (3+1)-dimensional Painlevé integrable equation [21]. We apply Painlevé analysis on the Kairat-X model to find the model is integrable. Then, we proceed to apply the Hirota bilinear method to derive exact soliton solutions. The Hirota Bilinear Method is one of the most graceful and powerful techniques in soliton theory; it is a direct method to construct soliton solutions by transforming a nonlinear PDE into bilinear form. This method is also used in distinct equations such as the fifth-order KdV-type equation [22], the nonlocal reverse space-time mKdV equation [23], the generalized coupled higher-order nonlinear Schrödinger equations [24], the Korteweg–de Vries equation [25], the (2+1)-dimensional Hirota–Satsuma–Ito equation [26], the (4+1)-dimensional BLMP equation [27], the generalized (2+1)-dimensional Hirota bilinear equation [28], the Fractional Sawada-Kotera Equation [29], the generalized perturbed KdV equation [30], and nonlinear partial differential equations [31].

Our primary objective of this work is to apply Painlevé analysis to examine the integrability of the Kairat-X equation and to derive novel analytical solutions, including breather waves, new periodic waves, periodic cross-kink waves, kink-rogue wave interactions, and one-soliton and two-soliton solutions, by employing the Hirota bilinear method. The machine learning multi-layer-perceptron regressor algorithm is applied to represent the behavior of the actual, and to predict the above solutions. Furthermore, we use asymptotic analysis to expect the physical demonstration of the graphs corresponding to the obtained soliton solutions.

This paper includes the following sections: Section 2: Sketch of Painlevé analysis and its outcomes; Section 3: Model's bilinearization; Section 4: Application of bilinear Hirota method; Section 5: Graphical representation; Section 6: Machine learning analysis; Section 7: Asymptotic analysis; and Section 8: Conclusions.

2. Sketch of Painlevé analysis

The Painlevé analysis is a test for the integrability of nonlinear partial differential equations (NLPDEs). It checks whether the only movable singularities of the solutions are poles. Consider a NLPDE:

$$\Phi(\Xi, \Xi_{\theta_1}, \Xi_{\theta_2}, \Xi_{\theta_1\theta_2}, \Xi_{\theta_1\theta_1}, \Xi_{\theta_2\theta_2}, ...) = 0. \tag{2.1}$$

The analysis is based on the assumption that the solution Ξ possesses a singularity manifold defined by

$$\Theta(\theta_1, \theta_2, ..., \theta_n) = 0. \tag{2.2}$$

The solution Ξ is then expanded as a generalized Laurent series about this singular manifold:

$$\Xi(\theta_1, \theta_2, ..., \theta_n) = \Theta^{\epsilon}(\theta_1, \theta_2, ..., \theta_n) \sum_{i=0}^{\infty} \Xi_i(\theta_1, \theta_2, ..., \theta_n)\Theta^i(\theta_1, \theta_2, ..., \theta_n), \tag{2.3}$$

where $\Xi_i(\boldsymbol{\theta})$ (for $i = 0, 1, 2, \dots$) and $\Theta(\boldsymbol{\theta})$ are arbitrary analytic functions, and ϵ is a negative integer (the leading-order exponent).

The Painlevé analysis proceeds in the following steps:

Step 1: The dominant terms in the NLPDE are identified by substituting the leading-order behavior of the series,

$$\Xi = \Theta^{\epsilon}\Xi_0 \tag{2.4}$$

into the NLPDE (2.1). By balancing the terms of the lowest power in Θ, an algebraic equation for the exponent ϵ is obtained, and ϵ must be a negative integer.

Step 2: Once ϵ is found, substituting the leading-order term (2.4) into the NLPDE and setting the coefficient of the lowest power of Θ to zero yields an equation for the non-zero leading coefficient Ξ_0. This equation often contains derivatives of Θ.

Step 3: The series expansion (2.3) is now substituted into the full NLPDE (2.1). This results in a sequence of equations for the coefficients Ξ_i. For coefficient Ξ_i, the equation typically takes the form:

$$L(\Xi_0, \Theta)\Xi_i = F(\Xi_0, \ldots, \Xi_{i-1}, \Theta), \tag{2.5}$$

where L is a linear differential operator acting on Ξ_i. The values of the index i for which the determinant of operator L vanishes (i.e., when L is singular) are called the resonance values denoted by $i = r_1, r_2, \ldots$. These values indicate the locations in the series where arbitrary functions can be introduced. The equation for the resonance values is found by considering the coefficient of Ξ_i in the equation for $\Theta^{i+\epsilon}$.

Step 4: The NLPDE is said to pass the Painlevé test if the number of arbitrary functions introduced (the Ξ_i coefficients and Θ) matches the order of the NLPDE. Specifically, at each positive integer resonance value $i = r$, the right-hand side of the equation for Ξ_r, $F(\Xi_0, \ldots, \Xi_{r-1}, \Theta)$, must vanish identically. These are the compatibility conditions or solvability conditions.

Step 5: If all conditions are met, namely, the leading-order exponent ϵ is a negative integer, and the compatibility conditions are satisfied at all positive integer resonance values, then the NLPDE (2.1) is considered to possess the Painlevé property and is a Painlevé integrable system.

2.1. Painlevé analysis on the Kairat-X equation

In this section, we detail the application of the Painlevé analysis to the nonlinear differential Kairat-X equation (denoted as Eq (1.1) in the original context, though the equation is not explicitly given here). The analysis assumes a solution with a singular manifold $\Theta(x, t) = 0$,

$$\Theta(x, t) = 0. \tag{2.6}$$

To determine the leading-order exponent ϵ and the coefficient Ξ_0, we substitute the dominant term $\Xi \approx \Xi_0\Theta^\epsilon$ (compare with Eq (2.4)) into the Kairat-X equation. By balancing the terms of the lowest power in Θ, the following values are obtained:

$$\epsilon = -1, \quad \Xi_0 = -2\Theta_x. \tag{2.7}$$

Substituting the full Laurent series expansion (2.3) into the Kairat-X equation and collecting terms of the same power in Θ yields a set of equations for the coefficients Ξ_i. The indices i for which the coefficient Ξ_i becomes arbitrary (due to the vanishing of the linear operator coefficient) are the resonance values. These values are

$$i = -3, -1, 2, 4.$$

The resonance at $i = -1$ is always associated with the arbitrary nature of the singular manifold $\Theta(x, t)$, and the negative values $i = -3, -1$ are not physical in this context. The positive integer resonances are $i = 2$ and $i = 4$.

The maximum positive resonance is $r_{\max} = 4$. Based on this, the Laurent series is truncated up to the Ξ_4 term::

$$\Xi = \Xi_0\Theta^{-1} + \Xi_1 + \Xi_2\Theta^1 + \Xi_3\Theta^2 + \Xi_4\Theta^3. \tag{2.8}$$

Putting Eq (2.8) into the Kairat-X equation yields the subsequent coefficients:

$$\Xi_1 = \frac{-2\Theta_t\Theta_{\rm xt} - \Theta_t\Theta_{\rm xxxx} - \Theta_{\rm tt}\Theta_x - 4\Theta_x\Theta_{\rm xxxt} + 2\Theta_{\rm xt}\Theta_{\rm xxx}}{12\Theta_t\Theta_x^3}. \tag{2.9}$$

$$\Xi_3 = \frac{-\Theta_t^3\Theta_{\rm tt}\Theta_x^2 - 2\Theta_t^4\Theta_x\Theta_{\rm xt}... - 6\Theta_t^3\Theta_x\Theta_{\rm xx}\Theta_{\rm xxxxx}}{144\Theta_t^3\Theta_x^7}. \tag{2.10}$$

The positive integer resonance values $i = 2$ and $i = 4$ indicate that the coefficients Ξ_2 and Ξ_4 must appear as arbitrary functions. The final step requires checking the compatibility conditions at $i = 2$ and $i = 4$. If the equations for Ξ_2 and Ξ_4 are satisfied identically when Ξ_2 and Ξ_4 are treated as arbitrary functions, the compatibility conditions hold. Since the provided outcomes state that Ξ_2 and Ξ_4 appear as arbitrary functions, and the compatibility conditions are thus satisfied, we conclude that the Kairat-X equation (1.1) possesses the Painlevé property and is deemed Painlevé integrable.

3. The model's bilinearization

The Hirota formula

$$\prod_{i=1}^{j} D_{\mu_i}^{n_i}\mathfrak{Q}.\,\xi = \prod_{i=1}^{j}\left(\frac{\partial}{\partial\mu_i} - \frac{\partial}{\partial\mu_i'}\right)^{n_i}\mathfrak{Q}(\mu_1,...,\mu_j)\xi(\mu_1',...,\mu_j')\Big|_{\mu_1=\mu_1',...,\mu_j=\mu_j'}. \tag{3.1}$$

Equation (1.1) converts into bilinear form through the transformation $u = -2(ln\mathfrak{Q})_x$,

$$-\ 2\mathfrak{Q}_t\mathfrak{Q}_{\rm xxx} - 2\mathfrak{Q}_t^2 + 2\mathfrak{Q}\mathfrak{Q}_{\rm tt} - 6\mathfrak{Q}_x\mathfrak{Q}_{\rm xxt} + 6\mathfrak{Q}_{\rm xt}\mathfrak{Q}_{\rm xx} + 2\mathfrak{Q}\mathfrak{Q}_{\rm xxxt} = 0. \tag{3.2}$$

In the form of D-operators, it can be expressed as:

$$\left(D^2{}_t - 3D_tD^2{}_x + D_tD_x^3\right)\mathfrak{Q}.\mathfrak{Q} = 0. \tag{3.3}$$

4. Application of the bilinear Hirota method

4.1. Breather wave solution

Let the following ansatz for a breather wave solution [24] be

$$\begin{cases} \varsigma_1 = a_1t + x, \\ \varsigma_2 = a_2t + x, \\ \mathfrak{Q} = e^{-p_1\varsigma_1} + \kappa_1 cos(p\varsigma_2) + \kappa_2 e^{p_1\varsigma_1}. \end{cases} \tag{4.1}$$

Putting Eq (4.1) and their respective derivatives into Eq (3.2), we get the following algebraic system:

$$8a_2\kappa_1^2p^4 - 2a_2^2\kappa_1^2p^2 + 32a_1\kappa_2p_1^4 + 8a_1^2\kappa_2p_1^2 = 0,$$

$$2a_1\kappa_1 p_1 p^3 + 6a_2\kappa_1 p_1 p^3 - 6a_1\kappa_1 p_1^3 p - 2a_2\kappa_1 p_1^3 p - 4a_1 a_2\kappa_1 p_1 p = 0,$$
$$2a_2\kappa_1 p^4 - 2a_2^2\kappa_1 p^2 - 6a_1\kappa_1 p_1^2 p^2 - 6a_2\kappa_1 p_1^2 p^2 + 2a_1\kappa_1 p_1^4 + 2a_1^2\kappa_1 p_1^2 = 0,$$
$$-2a_1\kappa_1\kappa_2 p_1 p^3 - 6a_2\kappa_1\kappa_2 p_1 p^3 + 6a_1\kappa_1\kappa_2 p_1^3 p + 2a_2\kappa_1\kappa_2 p_1^3 p + 4a_1 a_2\kappa_1\kappa_2 p_1 p = 0,$$
$$2a_2\kappa_1\kappa_2 p^4 - 2a_2^2\kappa_1\kappa_2 p^2 - 6a_1\kappa_1\kappa_2 p_1^2 p^2 - 6a_2\kappa_1\kappa_2 p_1^2 p^2 + 2a_1\kappa_1\kappa_2 p_1^4 + 2a_1^2\kappa_1\kappa_2 p_1^2 = 0,$$

after symbolic computational calculations, we gain multiple solution sets, which are listed as follows:

Set 1:

$$\{a_1 = 3p^2 - p_1^2, a_2 = p^2 - 3p_1^2, \kappa_2 = \frac{\kappa_1^2 p^2\left(p^2 - 3p_1^2\right)}{4p_1^2\left(p_1^2 - 3p^2\right)}\}, \tag{4.2}$$

$$u(x,t) = -\frac{2\left(\kappa_2 p_1 e^{p_1((3p^2-p_1^2)t+x)} - \kappa_1 p\sin\left(p\left(\left(p^2-3p_1^2\right)t+x\right)\right) + p_1\left(-e^{-p_1((3p^2-p_1^2)t+x)}\right)\right)}{\kappa_2 e^{p_1((3p^2-p_1^2)t+x)} + \kappa_1\cos\left(p\left(\left(p^2-3p_1^2\right)t+x\right)\right) + e^{-p_1((3p^2-p_1^2)t+x)}}. \tag{4.3}$$

Set 2:

$$\{a_1 = \frac{4p^2}{3}, a_2 = -\frac{4ip^2}{3\sqrt{3}}, p_1 = -\frac{p}{\sqrt{3}}, \kappa_2 = \frac{1}{8}\left(-1+3i\sqrt{3}\right)\kappa_1^2\}, \tag{4.4}$$

$$u(x,t) = -\frac{2\left(\kappa_2 p_1 e^{p_1(a_1t+x)} - \kappa_1 p\sin\left(p\left(a_2t+x\right)\right) + p_1\left(-e^{p_1(-(a_1t+x))}\right)\right)}{\kappa_2 e^{p_1(a_1t+x)} + \kappa_1\cos\left(p\left(a_2t+x\right)\right) + e^{p_1(-(a_1t+x))}}. \tag{4.5}$$

Set 3:

$$\{a_1 = -\frac{4ip^2}{\sqrt{3}}, a_2 = -4p^2, p_1 = -\sqrt{3}p, \kappa_2 = \frac{i\kappa_1^2}{6\sqrt{3}-2i}\}, \tag{4.6}$$

$$u(x,t) = -\frac{2\left(\kappa_2 p_1 e^{p_1(a_1t+x)} - \kappa_1 p\sin\left(p\left(a_2t+x\right)\right) + p_1\left(-e^{p_1(-(a_1t+x))}\right)\right)}{\kappa_2 e^{p_1(a_1t+x)} + \kappa_1\cos\left(p\left(a_2t+x\right)\right) + e^{p_1(-(a_1t+x))}}. \tag{4.7}$$

Set 4:

$$\{a_1 = \frac{4}{49}\left(1+4i\sqrt{3}\right)p^2, a_2 = \frac{4}{343}\left(10-9i\sqrt{3}\right)p^2, p_1 = -\frac{1}{7}\sqrt{-i\left(4\sqrt{3}-i\right)p^2}, \kappa_1 = 0\}, \tag{4.8}$$

$$u(x,t) = -\frac{2\sqrt{-i\left(4\sqrt{3}-i\right)p^2}\left(-\kappa_2 + \exp\left(\frac{2}{7}\sqrt{-i\left(4\sqrt{3}-i\right)p^2}\left(x+\frac{4}{49}p^2\left(t+4i\sqrt{3}t\right)\right)\right)\right)}{7\left(\kappa_2 + \exp\left(\frac{2}{7}\sqrt{-i\left(4\sqrt{3}-i\right)p^2}\left(x+\frac{4}{49}p^2\left(t+4i\sqrt{3}t\right)\right)\right)\right)}. \tag{4.9}$$

4.2. New periodic solution

Assume the following ansatz for a Lump-kink solution [25]:

$$\begin{cases} \varsigma_1 = a_2t + a_1x + a_3, \\ \varsigma_2 = b_2t + b_1x + b_3, \\ \varsigma_3 = c_2t + c_1x + c_3, \\ \mathfrak{Q} = \kappa_1 e^{\varsigma_1} + e^{-\varsigma_1} + \kappa_2\cos(p\varsigma_2) + \kappa_3\cosh(\varsigma_3) + \kappa_4. \end{cases} \tag{4.10}$$

Putting Eq (4.10) and their respective derivatives into Eq (3.2), we get the following algebraic system:

$$8a_2^2\kappa_1 + 32a_1^3a_2\kappa_1 + 8b_1^3b_2\kappa_2^2p^4 - 2b_2^2\kappa_2^2p^2 - 2c_2^2\kappa_3^2 - 8c_1^3c_2\kappa_3^2 = 0,$$

$$
\begin{aligned}
-6b_1^2b_2c_1\kappa_2\kappa_3p^3 - 2b_1^3c_2\kappa_2\kappa_3p^3 + 2b_2c_1^3\kappa_2\kappa_3p + 6b_1c_1^2c_2\kappa_2\kappa_3p + 4b_2c_2\kappa_2\kappa_3p &= 0,\\
-6b_1b_2c_1^2\kappa_2\kappa_3p^2 - 6b_1^2c_1c_2\kappa_2\kappa_3p^2 + 2b_1^3b_2\kappa_2\kappa_3p^4 - 2b_2^2\kappa_2\kappa_3p^2 + 2c_2^2\kappa_2\kappa_3 + 2c_1^3c_2\kappa_2\kappa_3 &= 0,\\
16c_2c_1^3\kappa_3^2 + 4c_2^2\kappa_3^2 &= 0,\\
2a_2b_1^3\kappa_2p^3 + 6a_1b_1^2b_2\kappa_2p^3 - 6a_1^2a_2b_1\kappa_2p - 2a_1^3b_2\kappa_2p - 4a_2b_2\kappa_2p &= 0,\\
-6a_1a_2b_1^2\kappa_2p^2 - 6a_1^2b_1b_2\kappa_2p^2 + 2a_2^2\kappa_2 + 2a_1^3a_2\kappa_2 + 2b_1^3b_2\kappa_2p^4 - 2b_2^2\kappa_2p^2 &= 0,\\
2a_1^3c_2\kappa_3 + 6a_2a_1^2c_1\kappa_3 + 6a_1c_1^2c_2\kappa_3 + 2a_2c_1^3\kappa_3 + 4a_2c_2\kappa_3 &= 0,\\
6a_1^2c_1c_2\kappa_3 + 6a_2a_1c_1^2\kappa_3 + 2a_2a_1^3\kappa_3 + 2a_2^2\kappa_3 + 2c_2^2\kappa_3 + 2c_1^3c_2\kappa_3 &= 0,\\
2a_2a_1^3\kappa_4 + 2a_2^2\kappa_4 &= 0,\\
-2a_2b_1^3\kappa_1\kappa_2p^3 - 6a_1b_1^2b_2\kappa_1\kappa_2p^3 + 6a_1^2a_2b_1\kappa_1\kappa_2p + 2a_1^3b_2\kappa_1\kappa_2p + 4a_2b_2\kappa_1\kappa_2p &= 0,\\
-6a_1a_2b_1^2\kappa_1\kappa_2p^2 - 6a_1^2b_1b_2\kappa_1\kappa_2p^2 + 2a_2^2\kappa_1\kappa_2 + 2a_1^3a_2\kappa_1\kappa_2 + 2b_1^3b_2\kappa_1\kappa_2p^4 - 2b_2^2\kappa_1\kappa_2p^2 &= 0,\\
-2a_1^3c_2\kappa_1\kappa_3 - 6a_2a_1^2c_1\kappa_1\kappa_3 - 6a_1c_1^2c_2\kappa_1\kappa_3 - 2a_2c_1^3\kappa_1\kappa_3 - 4a_2c_2\kappa_1\kappa_3 &= 0,\\
6a_1^2c_1c_2\kappa_1\kappa_3 + 6a_2a_1c_1^2\kappa_1\kappa_3 + 2a_2a_1^3\kappa_1\kappa_3 + 2a_2^2\kappa_1\kappa_3 + 2c_2^2\kappa_1\kappa_3 + 2c_1^3c_2\kappa_1\kappa_3 &= 0,\\
2a_2a_1^3\kappa_1\kappa_4 + 2a_2^2\kappa_1\kappa_4 &= 0,\\
2b_1^3b_2\kappa_2\kappa_4p^4 - 2b_2^2\kappa_2\kappa_4p^2 &= 0,\\
2c_2c_1^3\kappa_3\kappa_4 + 2c_2^2\kappa_3\kappa_4 &= 0,
\end{aligned}
$$

after symbolic computational calculations, we gain multiple solution sets, which are listed as follows:

Set 1:

$$\{a_1 = -ib_1p, a_2 = -4ib_1^3p^3, b_2 = 4b_1^3p^2, c_1 = -ib_1p, c_2 = -4ib_1^3p^3, \kappa_4 = 0\}, \tag{4.11}$$

$$u(x,t) = -\frac{2\left(ib_1pe^{-a_3+4ib_1^3p^3t+ib_1px} - b_1\kappa_3p\sin\left(4b_1^3p^3t + b_1px + ic_3\right) - b_1\kappa_2p\sin\left(p\left(4b_1^3p^2t + b_1x + b_3\right)\right)\right)}{e^{-a_3+4ib_1^3p^3t+ib_1px} + \kappa_3\cos\left(4b_1^3p^3t + b_1px + ic_3\right) + \kappa_2\cos\left(p\left(4b_1^3p^2t + b_1x + b_3\right)\right)}. \tag{4.12}$$

Set 2:

$$\{a_1 = ib_1p, a_2 = 4ib_1^3p^3, b_2 = 4b_1^3p^2, c_1 = ib_1p, c_2 = 4ib_1^3p^3, \kappa_4 = 0\}, \tag{4.13}$$

$$u(x,t) = -\frac{2b_1p(i\kappa_1e^{a_3+ib_1p(4b_1^2p^2t+x)} - ie^{-a_3-ib_1p(4b_1^2p^2t+x)} - \kappa_3\sin(4b_1^3p^3t + b_1px - ic_3) - \kappa_2\sin(p(4b_1^3p^2t + b_1x + b_3)))}{\kappa_1e^{a_3+ib_1p(4b_1^2p^2t+x)} + e^{-a_3-ib_1p(4b_1^2p^2t+x)} + \kappa_3\cos(4b_1^3p^3t + b_1px - ic_3) + \kappa_2\cos(p(4b_1^3p^2t + b_1x + b_3))}. \tag{4.14}$$

4.3. New periodic cross-kink wave solution

Let the following ansatz for a rogue wave solution [25] be

$$\begin{cases} \varsigma_1 = a_2t + a_1x + a_3,\\ \varsigma_2 = b_2t + b_1x + b_3,\\ \varsigma_3 = c_2t + c_1x + c_3,\\ \mathfrak{Q} = \kappa_1e^{\varsigma_1} + e^{-\varsigma_1} + \kappa_2\sin(p\varsigma_2) + \kappa_3\sinh(\varsigma_3) + \kappa_4. \end{cases} \tag{4.15}$$

Putting Eq (4.15) and their respective derivatives into Eq (3.2), we get the following algebraic system:

$$8a_2^2\kappa_1 + 32a_1^3a_2\kappa_1 + 8b_1^3b_2\kappa_2^2p^4 - 2b_2^2\kappa_2^2p^2 - 2c_2^2\kappa_3^2 - 8c_1^3c_2\kappa_3^2 = 0,$$

$$
\begin{aligned}
6b_1^2b_2c_1\kappa_2\kappa_3p^3+2b_1^3c_2\kappa_2\kappa_3p^3-2b_2c_1^3\kappa_2\kappa_3p-6b_1c_1^2c_2\kappa_2\kappa_3p-4b_2c_2\kappa_2\kappa_3p&=0,\\
-6b_1b_2c_1^2\kappa_2\kappa_3p^2-6b_1^2c_1c_2\kappa_2\kappa_3p^2+2b_1^3b_2\kappa_2\kappa_3p^4-2b_2^2\kappa_2\kappa_3p^2+2c_2^2\kappa_2\kappa_3+2c_1^3c_2\kappa_2\kappa_3&=0,\\
16c_2c_1^3\kappa_3^2+4c_2^2\kappa_3^2&=0,\\
-2a_2b_1^3\kappa_2p^3-6a_1b_1^2b_2\kappa_2p^3+6a_1^2a_2b_1\kappa_2p+2a_1^3b_2\kappa_2p+4a_2b_2\kappa_2p&=0,\\
-6a_1a_2b_1^2\kappa_2p^2-6a_1^2b_1b_2\kappa_2p^2+2a_2^2\kappa_2+2a_1^3a_2\kappa_2+2b_1^3b_2\kappa_2p^4-2b_2^2\kappa_2p^2&=0,\\
2a_1^3c_2\kappa_3+6a_2a_1^2c_1\kappa_3+6a_1c_1^2c_2\kappa_3+2a_2c_1^3\kappa_3+4a_2c_2\kappa_3&=0,\\
6a_1^2c_1c_2\kappa_3+6a_2a_1c_1^2\kappa_3+2a_2a_1^3\kappa_3+2a_2^2\kappa_3+2c_2^2\kappa_3+2c_1^3c_2\kappa_3&=0,\\
2a_2a_1^3\kappa_4+2a_2^2\kappa_4&=0,\\
2a_2b_1^3\kappa_1\kappa_2p^3+6a_1b_1^2b_2\kappa_1\kappa_2p^3-6a_1^2a_2b_1\kappa_1\kappa_2p-2a_1^3b_2\kappa_1\kappa_2p-4a_2b_2\kappa_1\kappa_2p&=0,\\
-6a_1a_2b_1^2\kappa_1\kappa_2p^2-6a_1^2b_1b_2\kappa_1\kappa_2p^2+2a_2^2\kappa_1\kappa_2+2a_1^3a_2\kappa_1\kappa_2+2b_1^3b_2\kappa_1\kappa_2p^4-2b_2^2\kappa_1\kappa_2p^2&=0,\\
-2a_1^3c_2\kappa_1\kappa_3-6a_2a_1^2c_1\kappa_1\kappa_3-6a_1c_1^2c_2\kappa_1\kappa_3-2a_2c_1^3\kappa_1\kappa_3-4a_2c_2\kappa_1\kappa_3&=0,\\
6a_1^2c_1c_2\kappa_1\kappa_3+6a_2a_1c_1^2\kappa_1\kappa_3+2a_2a_1^3\kappa_1\kappa_3+2a_2^2\kappa_1\kappa_3+2c_2^2\kappa_1\kappa_3+2c_1^3c_2\kappa_1\kappa_3&=0,\\
2a_2a_1^3\kappa_1\kappa_4+2a_2^2\kappa_1\kappa_4&=0,\\
2b_1^3b_2\kappa_2\kappa_4p^4-2b_2^2\kappa_2\kappa_4p^2&=0,\\
2c_2c_1^3\kappa_3\kappa_4+2c_2^2\kappa_3\kappa_4&=0,
\end{aligned}
$$

after symbolic computational calculations, we gain multiple solution sets, which are listed as follows:

Set 1:

$$\{a_1=ib_1p, a_2=4ib_1^3p^3, b_2=4b_1^3p^2, c_1=ib_1p, c_2=4ib_1^3p^3, \kappa_4=0\}, \tag{4.16}$$

$$u(x,t) = -\frac{2\left((-i)b_1pe^{-a_3-4ib_1^3p^3t-ib_1px}+ib_1\kappa_3p\cos\left(4b_1^3p^3t+b_1px-ic_3\right)+b_1\kappa_2p\cos\left(p\left(4b_1^3p^2t+b_1x+b_3\right)\right)\right)}{e^{-a_3-4ib_1^3p^3t-ib_1px}+i\kappa_3\sin\left(4b_1^3p^3t+b_1px-ic_3\right)+\kappa_2\sin\left(p\left(4b_1^3p^2t+b_1x+b_3\right)\right)}. \tag{4.17}$$

Set 2:

$$\{a_1=-ib_1p, a_2=-4ib_1^3p^3, b_2=4b_1^3p^2, c_1=ib_1p, c_2=4ib_1^3p^3, \kappa_4=0\}, \tag{4.18}$$

$$u(x,t) = -\frac{2(-ib_1\kappa_1pe^{a_3-4ib_1^3p^3t-ib_1px}+ib_1pe^{-a_3+4ib_1^3p^3t+ib_1px}+ib_1\kappa_3p\cos(4b_1^3p^3t+b_1px-ic_3)+b_1\kappa_2p\cos(p(4b_1^3p^2t+b_1x+b_3)))}{\kappa_1e^{a_3-4ib_1^3p^3t-ib_1px}+e^{-a_3+4ib_1^3p^3t+ib_1px}+i\kappa_3\sin(4b_1^3p^3t+b_1px-ic_3)+\kappa_2\sin(p(4b_1^3p^2t+b_1x+b_3))}. \tag{4.19}$$

4.4. The interaction between kink solitary wave and rogue wave solutions

Assume the following ansatz for an interaction between Kink solitary wave and rogue wave solutions [27]:

$$\begin{cases}\varsigma_1=b_1t+a_1x,\\ \varsigma_2=a_2x^2+b_2t^2,\\ \varsigma_3=b_3t+a_3x,\\ \mathfrak{Q}=(\varsigma_1)^2+(\varsigma_2)+\kappa e^{\varsigma_3}+1.\end{cases} \tag{4.20}$$

Putting Eq (4.20) and their respective derivatives into Eq (3.2), we get the following algebraic system:

$$24a_1^3b_1+24a_2a_1b_1+4b_1^2+4b_2=0,$$

$$
\begin{aligned}
-4a_3^3b_1^2\kappa - 4a_3^3b_2\kappa - 12a_1a_3^2b_1b_3\kappa - 8b_1^2b_3\kappa - 8b_2b_3\kappa &= 0,\\
2a_3^3b_3\kappa + 12a_1a_3^2b_1\kappa + 12a_1^2a_3b_3\kappa + 12a_2a_3b_3\kappa + 4b_1^2\kappa + 2b_3^2\kappa + 4b_2\kappa &= 0,\\
-4a_1^2b_1^2 + 4a_1^2b_2 + 4a_2b_1^2 + 4a_2b_2 &= 0,\\
2a_1^2a_3^3b_3\kappa + 2a_2a_3^3b_3\kappa + 2a_1^2b_3^2\kappa + 2a_2b_3^2\kappa &= 0,\\
-4b_1^4 - 8b_2b_1^2 - 4b_2^2 &= 0,\\
2a_3^3b_1^2b_3\kappa + 2a_3^3b_2b_3\kappa + 2b_1^2b_3^2\kappa + 2b_2b_3^2\kappa &= 0,\\
-4a_1a_3^3b_1\kappa - 12a_1^2a_3^2b_3\kappa - 12a_2a_3^2b_3\kappa - 8a_1b_1b_3\kappa &= 0,\\
-8a_1b_1^3 - 8a_1b_2b_1 &= 0,\\
4a_1a_3^3b_1b_3\kappa + 4a_1b_1b_3^2\kappa &= 0,
\end{aligned}
$$

after symbolic computational calculations, we gain multiple solution sets, which are listed as follows:
Set 1:

$$\{a_2 = -a_1^2, b_1 = 0, b_2 = 0, b_3 = -a_3^3\}. \tag{4.21}$$

Set 2:

$$\{a_1 = 0, a_2 = 0, b_2 = -b_1^2, b_3 = -a_3^3\}. \tag{4.22}$$

Both sets 1 and 2 give the same solution as the following:

$$u(x,t) = -\frac{2a_3\kappa e^{a_3x - a_3^3t}}{\kappa e^{a_3x - a_3^3t} + 1}. \tag{4.23}$$

4.5. 1-Soliton solution

Assume the following ansatz for a 1-Soliton wave solution [28]:

$$\begin{cases} \varsigma_1 = b_1t + a_1x, \\ \mathfrak{Q} = e^{\kappa(\varsigma_1)+\delta} + 1. \end{cases} \tag{4.24}$$

Putting Eq (4.24) and their respective derivatives into Eq (3.2), we get the following algebraic form:

$$2a_1^3b_1\kappa^4 + 2b_1^2\kappa^2 = 0,$$

after symbolic computational calculation, we gain a solution set, which is listed as follows:
Set 1:

$$\{a_1 = a_1, b_1 = a_1^3\left(-\kappa^2\right), \kappa = \kappa\}, \tag{4.25}$$

$$u(x,t) = -\frac{2a_1\kappa e^{\kappa\left(a_1x - a_1^3\kappa^2t\right)+\delta}}{e^{\kappa\left(a_1x - a_1^3\kappa^2t\right)+\delta} + 1}. \tag{4.26}$$

4.6. 2-Soliton solution

Assume the following ansatz for a 2-Soliton wave solution [28]:

$$\begin{cases} \varsigma_1 = b_1t + a_1x, \\ \varsigma_2 = b_2t + a_2x, \\ \mathfrak{Q} = e^{\kappa_1(\varsigma_1)+\delta_1} + e^{\kappa_2(\varsigma_2)+\delta_2} + Ae^{\kappa_1(\varsigma_1)+\delta_1+\kappa_2(\varsigma_2)+\delta_2} + 1. \end{cases} \tag{4.27}$$

Putting Eq (4.27) and their respective derivatives into Eq (3.2), we get the following algebraic system:

$$
\begin{aligned}
2a_2^3b_2\kappa_2^4 + 2b_2^2\kappa_2^2 = 0,\\
2a_2^3Ab_2\kappa_2^4 + 2Ab_2^2\kappa_2^2 = 0,\\
2a_1^3b_1\kappa_1^4 + 2b_1^2\kappa_1^2 = 0,\\
2a_1^3Ab_1\kappa_1^4 + 2Ab_1^2\kappa_1^2 = 0,\\
2a_1^3Ab_1\kappa_1^4 + 6a_1^2a_2Ab_1\kappa_2\kappa_1^3 + 2a_1^3Ab_2\kappa_2\kappa_1^3 + 6a_1a_2^2Ab_1\kappa_2^2\kappa_1^2 + 6a_1^2a_2Ab_2\kappa_2^2\kappa_1^2 + 2a_2^3Ab_1\kappa_2^3\kappa_1 + 6a_1a_2^2Ab_2\kappa_2^3\kappa_1 + 2a_2^3Ab_2\kappa_2^4 + 2a_1^3b_1\kappa_1^4\\
-6a_1^2a_2b_1\kappa_2\kappa_1^3 - 2a_1^3b_2\kappa_2\kappa_1^3 + 6a_1a_2^2b_1\kappa_2^2\kappa_1^2 + 6a_1^2a_2b_2\kappa_2^2\kappa_1^2 - 2a_2^3b_1\kappa_2^3\kappa_1 - 6a_1a_2^2b_2\kappa_2^3\kappa_1 + 2a_2^3b_2\kappa_2^4 + 2Ab_1^2\kappa_1^2 + 4Ab_1b_2\kappa_2\kappa_1\\
+2Ab_2^2\kappa_2^2 + 2b_1^2\kappa_1^2 - 4b_1b_2\kappa_2\kappa_1 + 2b_2^2\kappa_2^2 = 0,
\end{aligned}
$$

after symbolic computational calculations, we gain multiple solution sets, which are listed as follows:

Set 1:

$$\{b_1 = 0, b_2 = -a_2^3\kappa_2^2, A = \frac{a_1^2\kappa_1^2 - 3a_1a_2\kappa_2\kappa_1 + 3a_2^2\kappa_2^2}{a_1^2\kappa_1^2 + 3a_1a_2\kappa_2\kappa_1 + 3a_2^2\kappa_2^2}\}, \tag{4.28}$$

$$u(x,t) = -\frac{2\left(A\left(a_1\kappa_1 + a_2\kappa_2\right)\exp\left(\kappa_2\left(a_2x - a_2^3\kappa_2^2t\right) + a_1\kappa_1x + \delta_1 + \delta_2\right) + a_2\kappa_2e^{\kappa_2\left(a_2x - a_2^3\kappa_2^2t\right) + \delta_2} + a_1\kappa_1e^{a_1\kappa_1x + \delta_1}\right)}{A\exp\left(\kappa_2\left(a_2x - a_2^3\kappa_2^2t\right) + a_1\kappa_1x + \delta_1 + \delta_2\right) + e^{\kappa_2\left(a_2x - a_2^3\kappa_2^2t\right) + \delta_2} + e^{a_1\kappa_1x + \delta_1} + 1}. \tag{4.29}$$

Set 2:

$$\{b_1 = -a_1^3\kappa_1^2, b_2 = -a_2^3\kappa_2^2, A = \frac{\left(a_2\kappa_2 - a_1\kappa_1\right)^2\left(a_1^2\kappa_1^2 + a_1a_2\kappa_2\kappa_1 + a_2^2\kappa_2^2\right)}{\left(a_1\kappa_1 + a_2\kappa_2\right)^2\left(a_1^2\kappa_1^2 - a_1a_2\kappa_2\kappa_1 + a_2^2\kappa_2^2\right)}\}, \tag{4.30}$$

$$u(x,t) = -\frac{2(A(a_1\kappa_1 + a_2\kappa_2)\exp(\kappa_1(a_1x - a_1^3\kappa_1^2t) + \kappa_2(a_2x - a_2^3\kappa_2^2t) + \delta_1 + \delta_2) + a_1\kappa_1e^{\kappa_1(a_1x - a_1^3\kappa_1^2t) + \delta_1} + a_2\kappa_2e^{\kappa_2(a_2x - a_2^3\kappa_2^2t) + \delta_2})}{A\exp(\kappa_1(a_1x - a_1^3\kappa_1^2t) + \kappa_2(a_2x - a_2^3\kappa_2^2t) + \delta_1 + \delta_2) + e^{\kappa_1(a_1x - a_1^3\kappa_1^2t) + \delta_1} + e^{\kappa_2(a_2x - a_2^3\kappa_2^2t) + \delta_2} + 1}. \tag{4.31}$$

Set 3:

$$\{b_1 = -a_1^3\kappa_1^2, b_2 = 0, A = \frac{3a_1^2\kappa_1^2 - 3a_1a_2\kappa_2\kappa_1 + a_2^2\kappa_2^2}{3a_1^2\kappa_1^2 + 3a_1a_2\kappa_2\kappa_1 + a_2^2\kappa_2^2}\}, \tag{4.32}$$

$$u(x,t) = -\frac{2\left(A\left(a_1\kappa_1 + a_2\kappa_2\right)\exp\left(\kappa_1\left(a_1x - a_1^3\kappa_1^2t\right) + a_2\kappa_2x + \delta_1 + \delta_2\right) + a_1\kappa_1e^{\kappa_1\left(a_1x - a_1^3\kappa_1^2t\right) + \delta_1} + a_2\kappa_2e^{a_2\kappa_2x + \delta_2}\right)}{A\exp\left(\kappa_1\left(a_1x - a_1^3\kappa_1^2t\right) + a_2\kappa_2x + \delta_1 + \delta_2\right) + e^{\kappa_1\left(a_1x - a_1^3\kappa_1^2t\right) + \delta_1} + e^{a_2\kappa_2x + \delta_2} + 1}. \tag{4.33}$$

5. Graphical representation

Graphical representation by putting suitable values for the parameters in our analytical solutions illustrates various types of wave structures, including breather waves, new periodic waves, new periodic cross-kink waves, interactions between kink solitons and rogue waves, and 1-soliton and 2-soliton wave solutions. These are depicted in the following figures: In Figure 1, breather wave solution u(x,t) Eq (4.3) in (a) Abs(u) and (b) Re(u) are shown in 3-dim, contour, and 2-dim with $p_1 = 0.5, \kappa_1 = 2.1, q = 1.3$. In Figure 2, new periodic wave solution u(x,t) Eq (4.12) in (a) Abs(u) and (b) Re(u) are shown in 3-dim, contour, and 2-dim with $a_3 = 0, b_1 = 1.2, b_3 = 0, c_3 = 0, \kappa_2 = 2.5, \kappa_3 = 1.5, p = 1.1$, and $q = 1.3$. In Figure 3, new periodic cross-kink wave solution u(x,t) Eq (4.17) in (a) Abs(u) and (b) Re(u) are shown in 3-dim, contou,r and 2-dim with $a_3 = 1, b_1 = 1.2, b_3 = -1, c_3 = 1, \kappa_2 = 1.5, \kappa_3 = 0.5, p = 0.4$, and $q = 0.5$. In Figure 4, the interaction between kink solitary wave and rogue

wave solution u(x,t) Eq (4.23) in (a) Abs(u) and (b) Re(u) are shown in 3-dim, contour, and 2-dim with $a_3 = 1.5$ *and* $\kappa = -1.9$. In Figure 5, 1-Soliton wave solution u(x,t) Eq (4.26) in (a) Abs(u) and (b) Re(u) are shown in 3-dim, contour, and 2-dim with $a_1 = -1.2, \kappa = 2.2$ and $\delta = 0.2$. In Figure 6, 2-Soliton wave solution u(x,t) Eq (4.29) in (a) Abs(u) and (b) Re(u) are shown in 3-dim, contour, and 2-dim with $a_1 = -1.5, \kappa_1 = 1.5, \delta_1 = 0.2, a_2 = 1.9, \kappa_2 = 2.3$ and $\delta_2 = 0.5$.

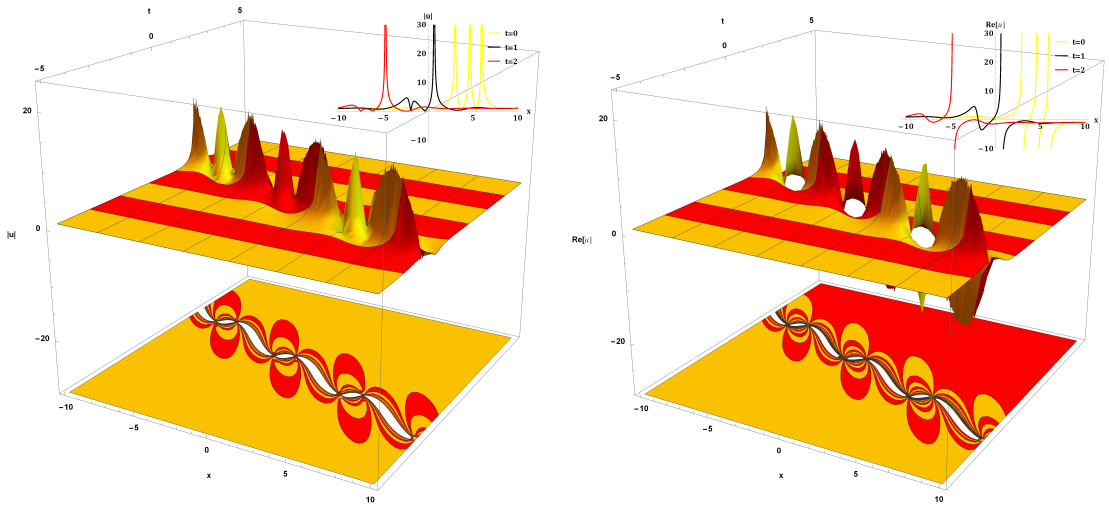

(a) (b)

Figure 1. Breather wave behavior of the solution is illustrated in Eq (4.3).

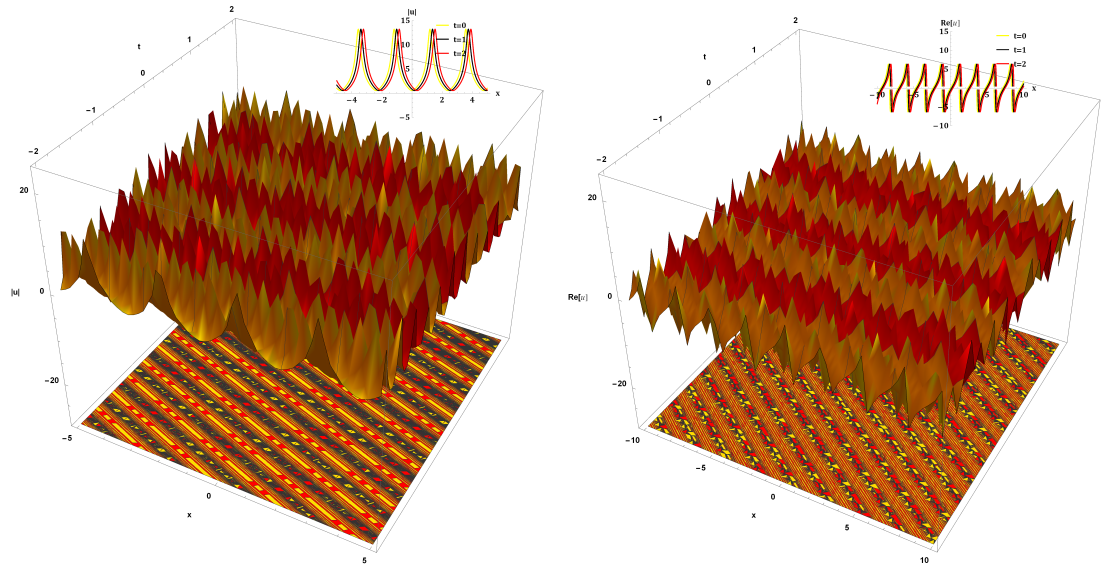

(a) (b)

Figure 2. New periodic wave behavior of solution appearance in Eq (4.12).

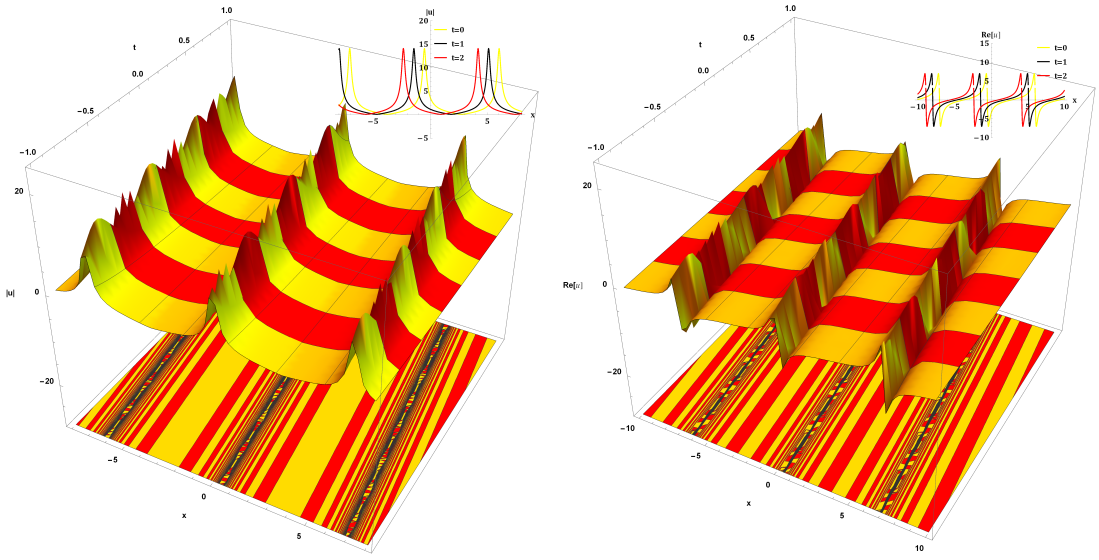

(a) (b)

Figure 3. New periodic Cross-Kink wave behavior of the solution is presented in Eq (4.17).

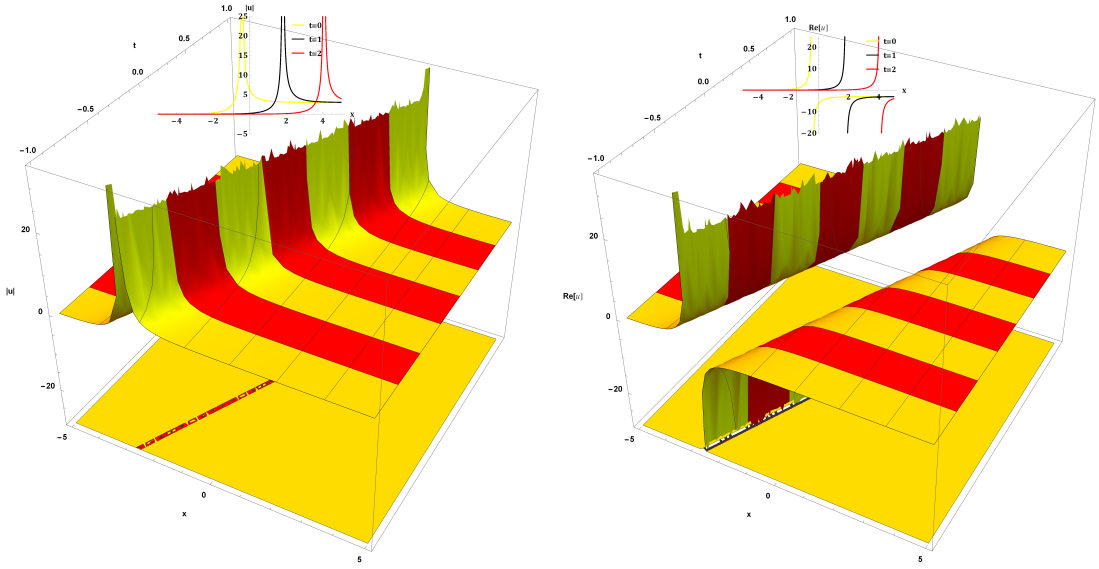

(a) (b)

Figure 4. The interaction between Kink solitary wave and rogue wave behavior of the solution is presented in Eq (4.23).

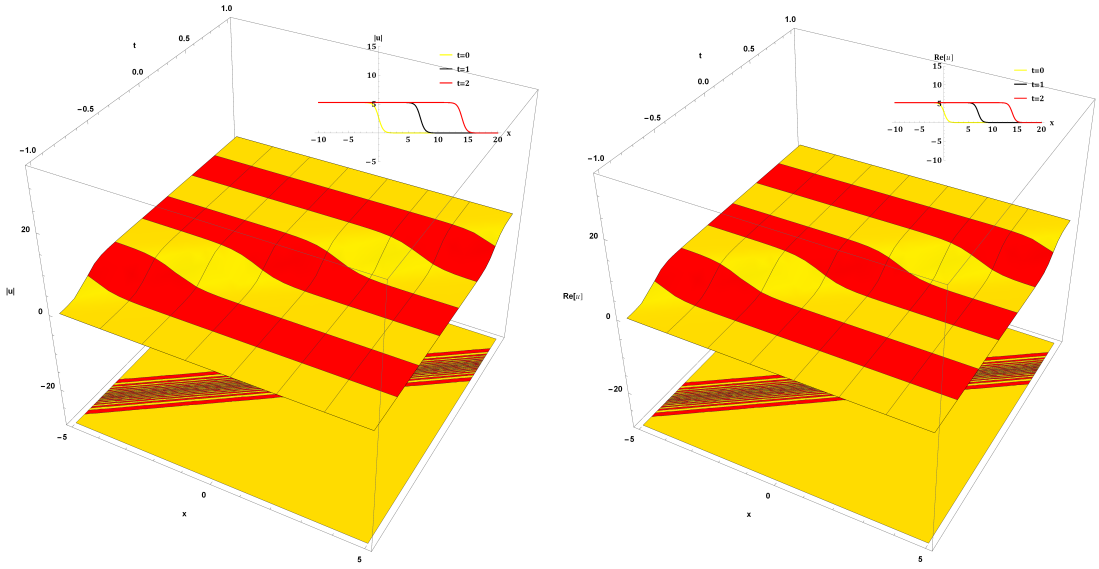

(a) (b)

Figure 5. 1-Soliton wave behavior of the solution is presented in Eq (4.26).

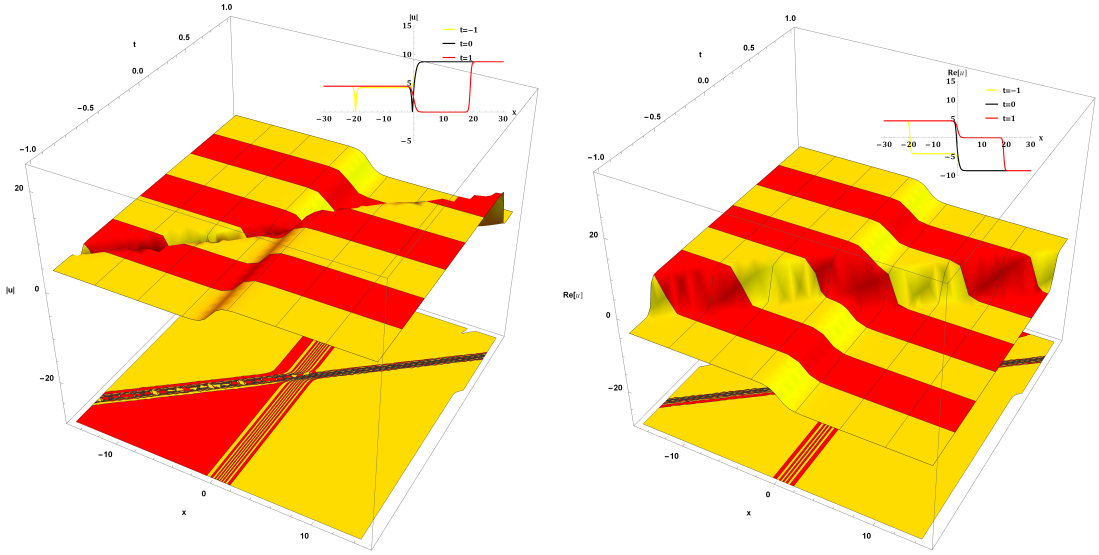

(a) (b)

Figure 6. 2-Soliton wave behavior of the solution is presented in Eq (4.29).

6. Machine learning

Here, we use the machine learning MLP regressor algorithm, which consists of one input and output with different hidden layers [32, 33]. Table 1 shows the configuration and training parameters of the algorithm.

Table 1. Neural network configuration and training parameters.

Parameter	Description
Data Split	80% training and 20% testing
Normalization Range	[0, 1]
Neural Network Structure	Input and output layers with multiple hidden layers
Propagation Method	Forward and backward propagation
Activation Function	Sigmoid
Optimization Algorithm	Gradient Descent
Loss Function	Mean Squared Error (MSE)
Learning Rate	0.1
Training Iterations	10,000 and 100,000 epochs
Implementation Tool	Python 3.13.1
Outputs	Actual vs. predicted plots and loss convergence

6.1. Results and discussion

In this section, we present and analyze three distinct types of solutions, the new periodic cross-kink, the one-soliton, and the two-soliton solutions, obtained for the problem under study. We then examine the agreement between their analytical (actual) results and the predicted results generated by a multilayer perceptron (MLP) regressor machine learning algorithm.

- Periodic cross-kink solution (Eq (4.17)):
  - Physical behavior: Illustrated in Figure 3.
  - MLP performance: The MLP regressor closely approximates the analytical solution, as visually confirmed by the comparison between actual and predicted data in Figure 7.
  - Training details: The model is trained for 100,000 epochs.
  - Metrics: Achieve a minimal mean squared error (MSE) loss, which is summarized in Table 2.
  - Computational time: The total prediction time is 106.738 seconds.
- One-soliton solution (Eq (4.26)):
  - Physical behavior: Presented in Figure 5.
  - MLP performance: The predicted results demonstrate excellent agreement with the actual analytical data, as shown in Figure 8.
  - Training details: The algorithm is trained for 10,000 epochs.
  - Metrics: The resulting MSE loss is reported in Table 3.
  - Computational time: The prediction is completed in 53.191 seconds.
- Two-soliton solution (Eq (4.29)):
  - Physical behavior: Depicted in Figure 6.
  - MLP performance: The MLP regressor produces results in close correspondence with the actual data, displayed in Figure 9.
  - Training details: Training is performed for 10,000 epochs.
  - Metrics: The obtained MSE loss is listed in Table 4.
  - Computational time: The total computation time for this case is 61.249 seconds.

In all three cases, the MLP regressor proves to be an effective tool for accurately predicting the analytical solutions, demonstrating its potential for approximating complex non-linear wave phenomena.

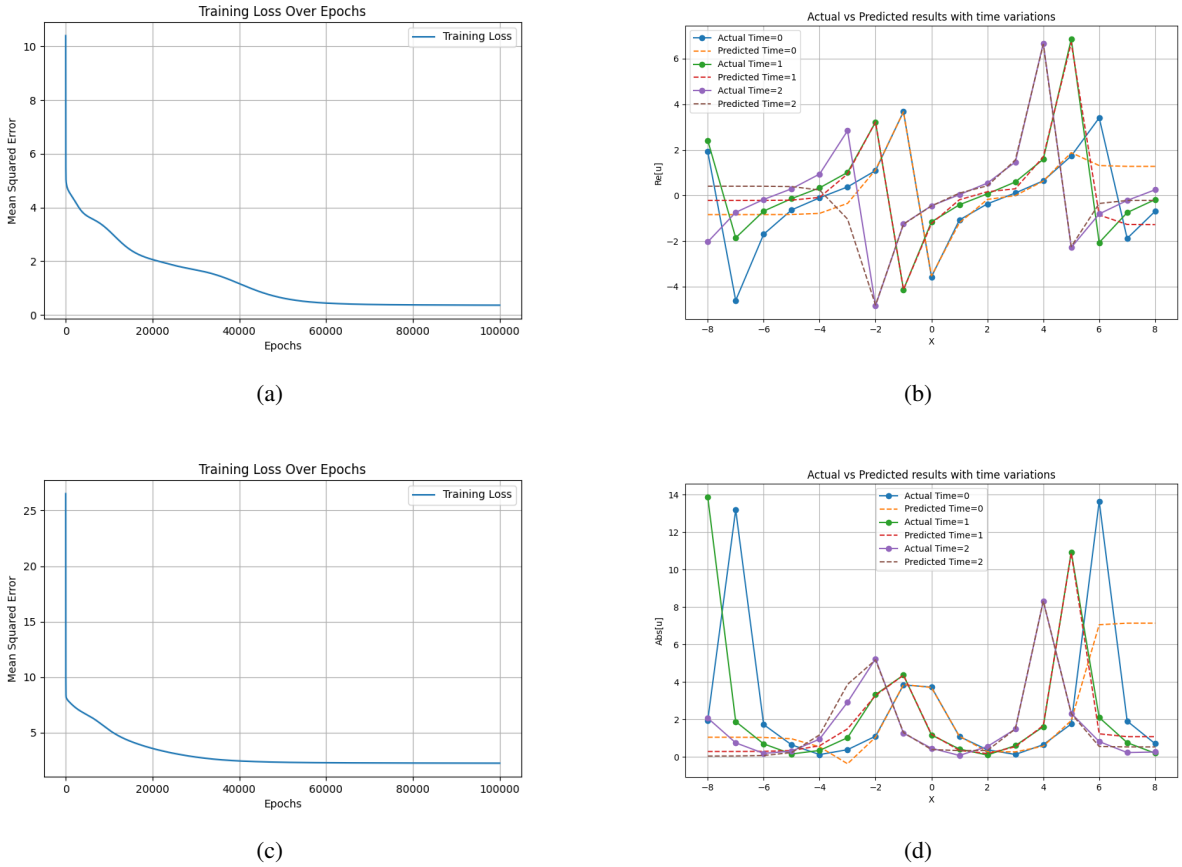

Figure 7. Actual and predicted behavior of the solution appearance in Eq (4.17).

Table 2. Epoch and loss during the prediction of solution Eq (4.17).

For Re[u] solution										
Epoch	10000	20000	30000	40000	50000	60000	70000	80000	90000	100000
Loss	3.1320	2.0616	1.6779	1.1656	0.6285	0.4405	0.3903	0.3742	0.3671	0.3632
For Abs[u] solution										
Epoch	10000	20000	30000	40000	50000	60000	70000	80000	90000	100000
Loss	5.2416	3.5760	2.7993	2.4498	2.3310	2.2892	2.2711	2.2610	2.2542	2.2491

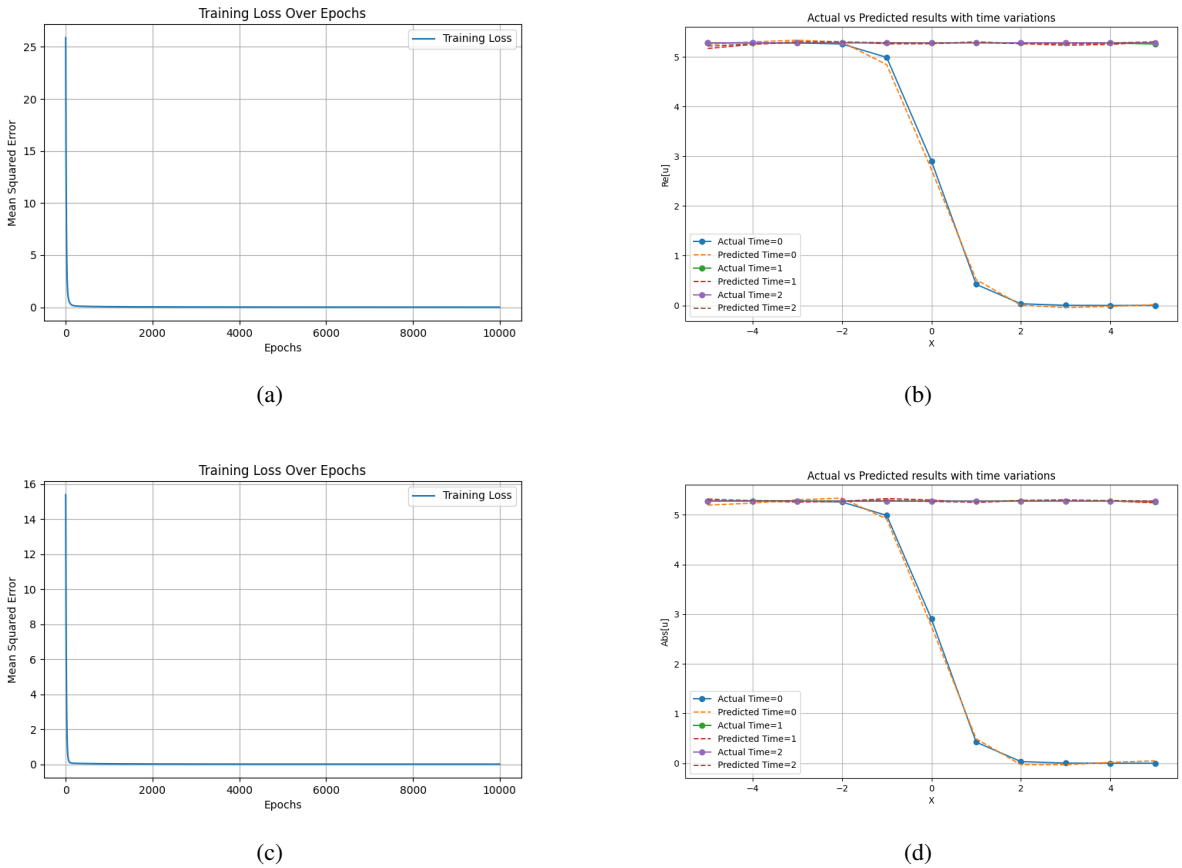

Figure 8. Actual and predicted behavior of the solution appearance in Eq (4.26).

Table 3. Epoch and loss during the prediction of solution Eq (4.26).

For Re[u] solution										
Epoch	1000	2000	3000	4000	5000	6000	7000	8000	9000	10000
Loss	0.0486	0.0262	0.0164	0.0110	0.0077	0.0056	0.0042	0.0032	0.0025	0.0020
For Abs[u] solution										
Epoch	1000	2000	3000	4000	5000	6000	7000	8000	9000	10000
Loss	0.0236	0.0120	0.0069	0.0044	0.0032	0.0025	0.0021	0.0018	0.0015	0.0013

Table 4. Epoch and loss during the prediction of solution Eq (4.29).

For Re[u] solution										
Epoch	1000	2000	3000	4000	5000	6000	7000	8000	9000	10000
Loss	1.8149	0.9199	0.686	0.5575	0.4563	0.3753	0.3293	0.3127	0.2990	0.2869
For Abs[u] solution										
Epoch	1000	2000	3000	4000	5000	6000	7000	8000	9000	10000
Loss	1.2110	0.9934	0.7461	0.5431	0.4050	0.3212	0.3049	0.2919	0.2801	0.2694

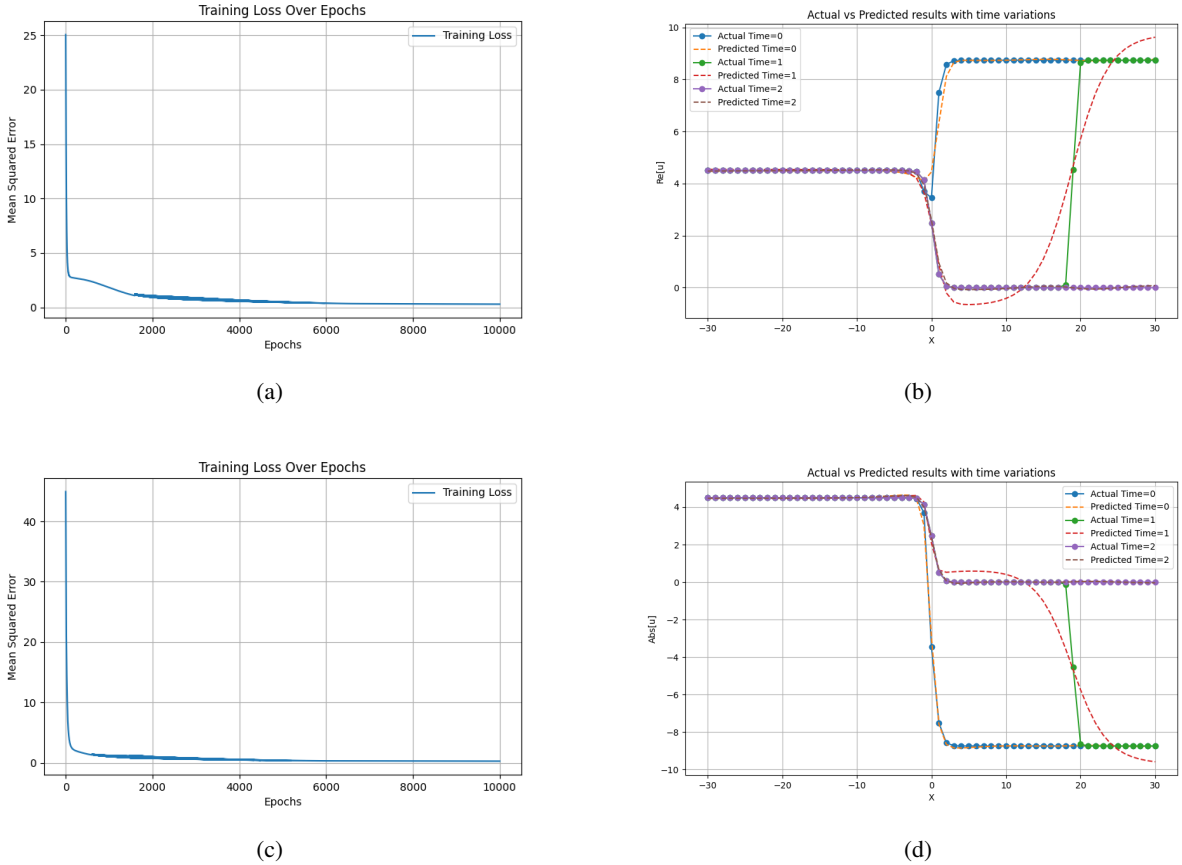

(a) (b)

(c) (d)

Figure 9. Actual and predicted behavior of the solution appearance in Eq (4.29).

7. Asymptotic analysis of the solutions

In this section, we describe the asymptotic analysis of the gained solutions. Figures 10–13 depict the asymptotic behavior of various solutions, as discussed in the following subsections. We aim to better understand the long-time dynamics of solution u(x, t) in Eq (4.3).

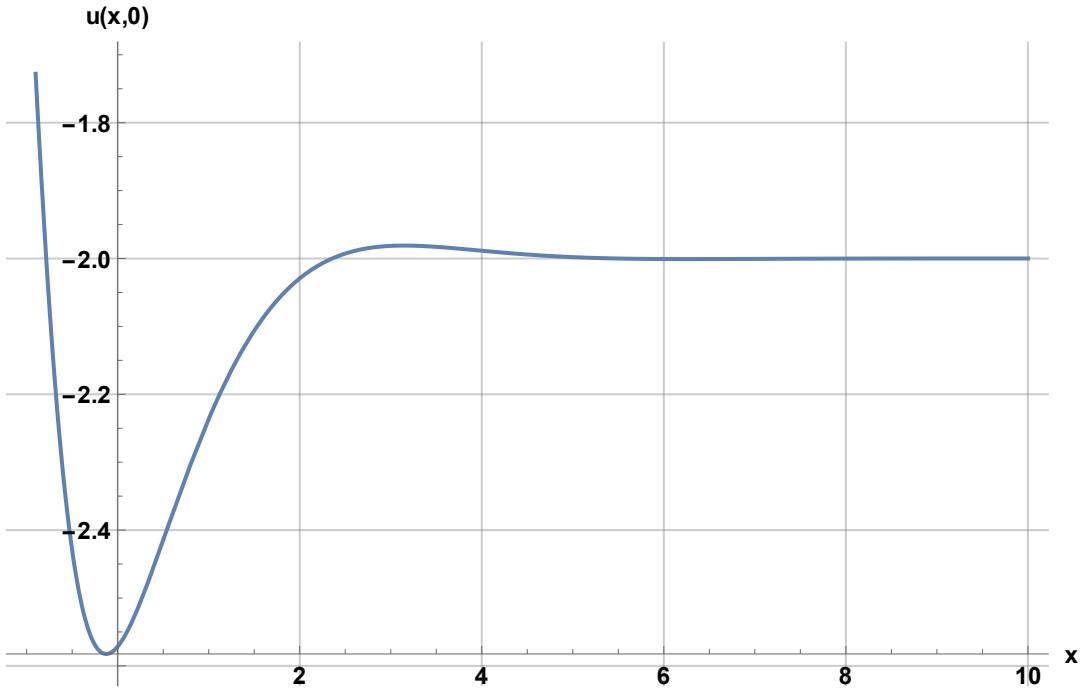

Figure 10. Asymptotic behavior of the solution presented in Eq (4.3).

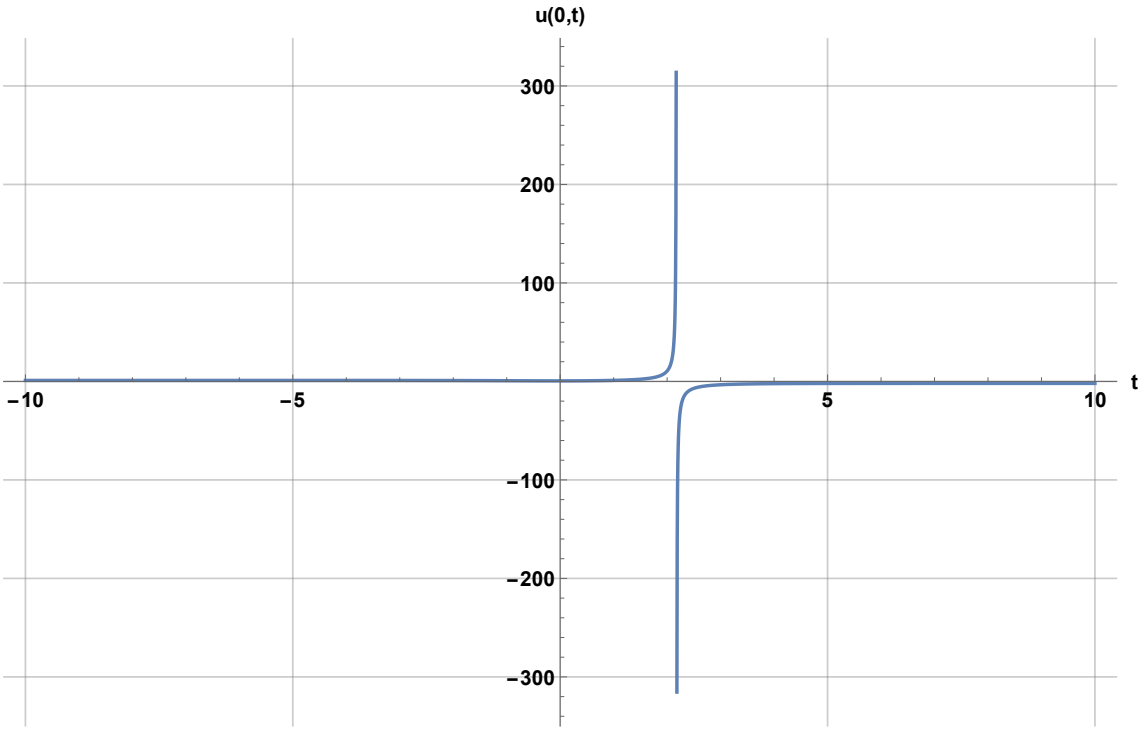

Figure 11. Asymptotic behavior of the solution presented in Eq (4.3).

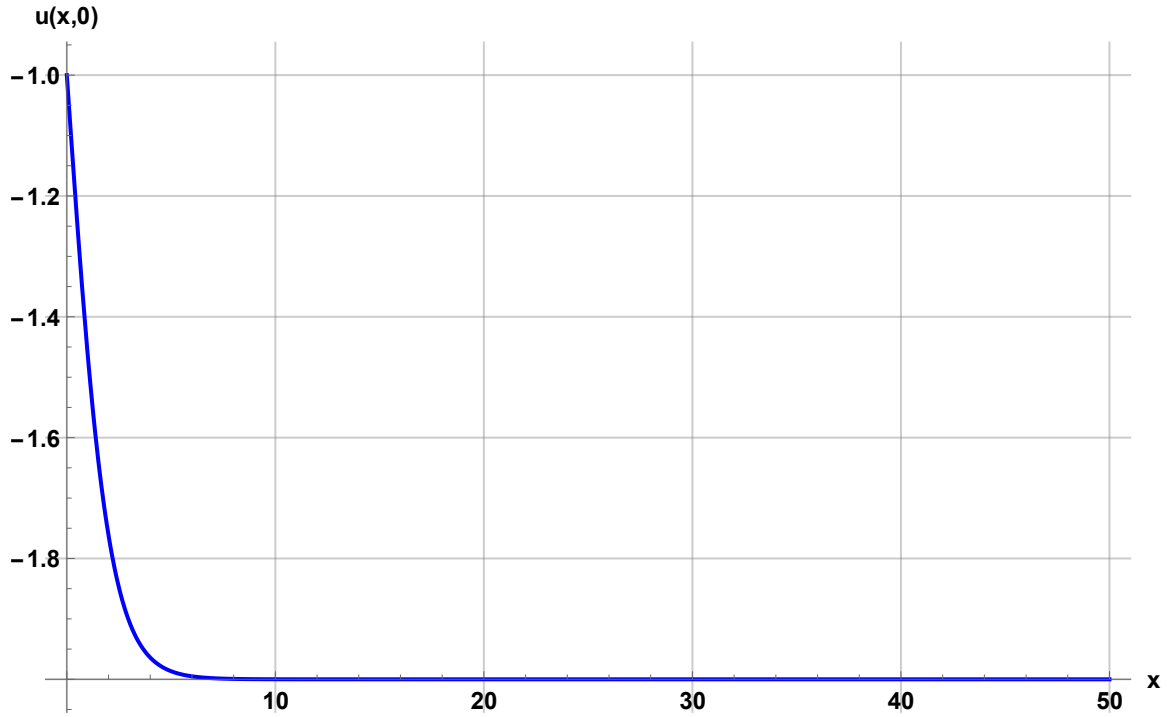

Figure 12. Asymptotic behavior of the solution presented in Eq (4.17).

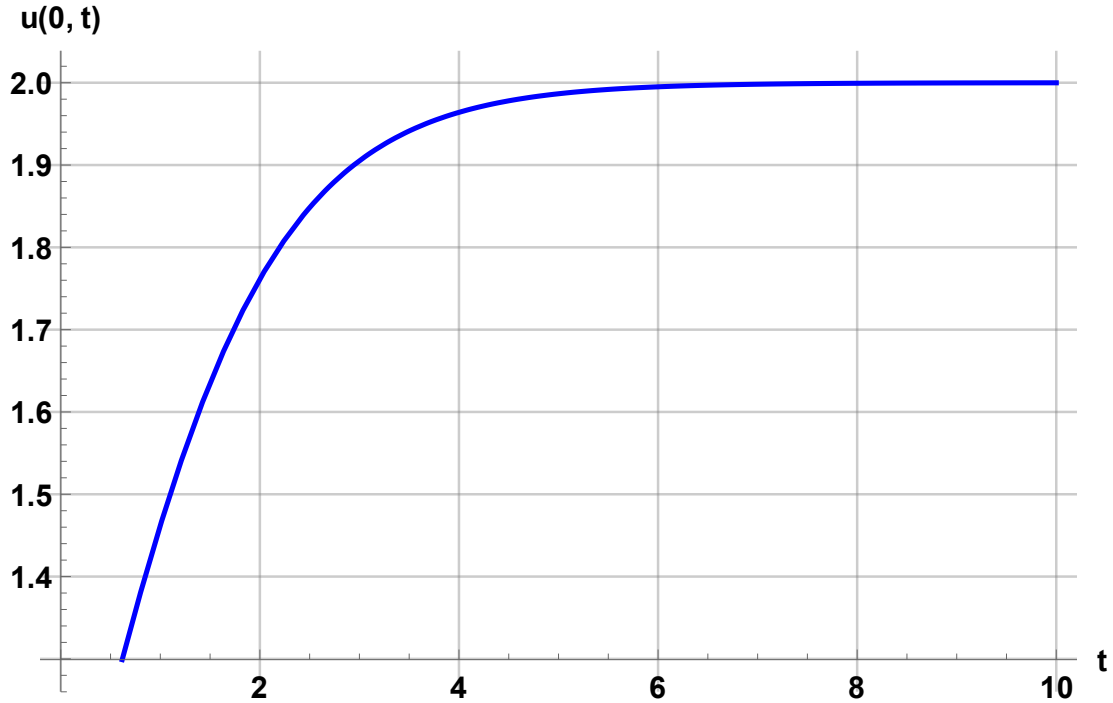

Figure 13. Asymptotic behavior of the solution presented in Eq (4.17).

7.1. Asymptotic behavior as $x \to \pm\infty$ at $t = 0$

At time $t = 0$, the solution becomes:

$$u(x,0) = -2 \cdot \frac{Ae^{-p_1 x} - \kappa_1 p \sin(px) - p_1 e^{-p_1 x}}{Ae^{-p_1 x} + \kappa_1 \cos(px) + e^{-p_1 x}}.$$

7.2. Asymptotic behavior as $t \to \pm\infty$ at $x = 0$

$$u(0,t) = -\frac{2\left(\dfrac{\kappa_1^2 p^2 (p^2 - 3p_1^2) e^{p_1(3p^2 - p_1^2)t}}{4p_1(p_1^2 - 3p^2)} - \kappa_1 p \sin\Big[p(p^2 - 3p_1^2)t\Big] - p_1 e^{-p_1(3p^2 - p_1^2)t}\right)}{\dfrac{\kappa_1^2 p^2 (p^2 - 3p_1^2) e^{p_1(3p^2 - p_1^2)t}}{4p_1^2(p_1^2 - 3p^2)} + \kappa_1 \cos\Big[p(p^2 - 3p_1^2)t\Big] + e^{-p_1(3p^2 - p_1^2)t}}. \tag{7.1}$$

This represents a transition from a constant state to a periodic nonlinear wave as time increases. Asymptotic analysis of solution u(x, t) in Eq (4.17).

7.3. Asymptotic behavior as $x \to \pm\infty$ at $t = 0$

$$u(x,0) = -\frac{2\Big((-i)b_1 p e^{-a_3 - ib_1 px} + ib_1\kappa_3 p \cos(b_1 px - ic_3) + b_1\kappa_2 p \cos(p(b_1 x + b_3))\Big)}{e^{-a_3 - ib_1 px} + i\kappa_3 \sin(b_1 px - ic_3) + \kappa_2 \sin(p(b_1 x + b_3))}. \tag{7.2}$$

This represents a traveling front moving in the positive x-direction, connecting the asymptotic states.

7.4. Asymptotic behavior as $t \to \pm\infty$ at $x = 0$

$$u(0,t) = -\frac{2\Big((-i)b_1 p e^{-a_3 - 4ib_1^3 p^3 t} + ib_1\kappa_3 p \cos(4b_1^3 p^3 t - ic_3) + b_1\kappa_2 p \cos(p(4b_1^3 p^2 t + b_3))\Big)}{e^{-a_3 - 4ib_1^3 p^3 t} + i\kappa_3 \sin(4b_1^3 p^3 t - ic_3) + \kappa_2 \sin(p(4b_1^3 p^2 t + b_3))}. \tag{7.3}$$

This confirms that the solution represents a decaying front in time at fixed spatial locations.

8. Conclusions

Through the combined application of Painlevé analysis and the bilinear Hirota method, we have entrenched the integrability and exact solvability of the newly proposed Kairat-X equation. By performing an attentive Painlevé test, we verified that the equation holds the Painlevé property. This integrability check validates the mathematical consistency of the problem and supports the application of strong analytical techniques to obtain exact solutions. Utilizing Hirota's bilinear formalism, we successfully transformed the nonlinear equation into a bilinear form and constructed breather wave, new periodic wave, new periodic cross-kink wave, the interaction between kink solitary and rogue wave, 1-Soliton wave and 2-Soliton wave solutions. These solutions display the distinctive characteristics of solitons, including shape preservation and elastic iterations upon impact. We executed asymptotic analysis on the gain solution to check the asymptotic behavior of the gained solutions. The machine learning multi-layer-perceptron regressor algorithm was successfully executed

to represent the behavior of the actual, and to predict, the above solutions. Furthermore, the analytical framework developed in this work holds significant potential for applications in other fields such as nonlinear fluid dynamics, optics, plasma physics, and other areas where solitonic phenomena show a vital role in demonstrating and understanding complex wave interactions. These findings suggest that the proposed model can be further explored in future research. The Painlevé analysis, being a widely adopted technique for assessing the integrability of nonlinear models, remains a valuable tool for such investigations. The obtained results were verified and validated using symbolic and numerical computations through Mathematica software. Additionally, several of the derived solutions are presented graphically using two-dimensional, three-dimensional, and contour plots to better convey their physical characteristics and behaviors.

Authors contributions

All authors of this article have been contributed equally. All authors have read and approved the final version of the manuscript for publication.

Use of Generative-AI tools declaration

The authors declare they have not used Artificial Intelligence (AI) tools in the creation of this article.

Acknowledgments

This work was supported by the Deanship of Scientific Research, Vice Presidency for Graduate Studies and Scientific Research, King Faisal University, Saudi Arabia.

Funding

This work was funded by the Deanship of Scientific Research, Vice Presidency for Graduate Studies and Scientific Research, King Faisal University, Saudi Arabia [KFU254545].

Conflict of interest

The authors declare no conflicts of interest.

References

1. Z. Myrzakulova, S. Manukure, R. Myrzakulov, G. Nugmanova, Integrability, geometry and wave solutions of some Kairat equations, 2025, arXiv:2307.00027. https://doi.org/10.48550/arXiv.2307.00027
2. Y. L. Xiao, S. Barak, M. Hleili, K. Shah, Exploring the dynamical behaviour of optical solitons in integrable kairat-II and kairat-X equations, *Phys. Scr.*, **99** (2024), 095261. https://doi.org/10.1088/1402-4896/ad6e34

3. A. M. Wazwaz, Extended (3+1)-dimensional Kairat-II and Kairat-X equations: Painlevé integrability, multiple soliton solutions, lump solutions, and breather wave solutions, *Int. J. Numer. Method. H.*, **34** (2024), 2177–2194. https://doi.org/10.1108/HFF-01-2024-0053
4. W. A. Faridi, G. H. Tipu, M. B. Riaz, A. M. Mostafa, S. A. AlQahtani, R. Myrzakulov, et al., Analyzing optical soliton solutions in Kairat-X equation via new auxiliary equation method, *Opt. Quant. Electron.*, **56** (2024), 1317. https://doi.org/10.1007/s11082-024-07197-7
5. M. Iqbal, D. C. Lu, A. R. Seadawy, F. A. H. Alomari, Z. Umurzakhova, R. Myrzakulov, Constructing the soliton wave structure to the nonlinear fractional Kairat-X dynamical equation under computational approach, *Mod. Phys. Lett. B*, **39** (2025), 2450396. https://doi.org/10.1142/S0217984924503962
6. M. Awadalla, A. Zafar, A. Taishiyeva, M. Raheel, Exact soliton solutions of M-fractional Kairat-II and Kairat-X equations via three analytical methods, in press. https://doi.org/10.13140/RG.2.2.18605.26080
7. T. Mathanaranjan, Lie symmetries, soliton solutions, conservation laws and stability analysis of the combined Kairat-II-X equation, *Math. Method. Appl. Sci.*, **48** (2025), 16722–16729. https://doi.org/10.1002/mma.70121
8. M. M. Al-Sawalha, S. Mukhtar, A. S. Alshehry, M. Alqudah, M. S. Aldhabani, Kink soliton phenomena of fractional conformable Kairat equations, *AIMS Mathematics*, **10** (2025), 2808–2828. https://doi.org/10.3934/math.2025131
9. M. N. Rafiq, M. H. Rafiq, H. Alsaud, Diversity of soliton dynamics, positive multi-complexiton solutions and modulation instability for (3+1)-dimensional extended Kairat-X equation, *Mod. Phys. Lett. B*, **39** (2025), 2550112. https://doi.org/10.1142/S021798492550112X
10. R. Qahiti, N. M. A. Alsafri, H. Zogan, A. A. Faqihi, Kink soliton solution of integrable Kairat-X equation via two integration algorithms, *AIMS Mathematics*, **9** (2024), 30153–30173. https://doi.org/10.3934/math.20241456
11. G. X. Li, Z. Y. Wang, K. Wang, N. Q. Jiang, G. M. Wei, Analytic investigation of a generalized variable-coefficient KdV equation with external-force term, *Mathemaics*, **13** (2025), 1642. https://doi.org/10.3390/math13101642
12. N. A. Kudryashov, S. F. Lavrova, Painlevé analysis of the traveling wave reduction of the third-order derivative nonlinear Schrödinger equation, *Mathematics*, **12** (2024), 1632. https://doi.org/10.3390/math12111632
13. H. D. Liu, B. Tian, C. D. Cheng, T. Y. Zhou, X. T. Gao, Painlevé analysis, bilinear forms, Bäcklund transformations and solitons for a variable-coefficient extended Korteweg-de vries equation with an external-force term in fluid mechanics and plasma dynamics, *Qual. Theory Dyn. Syst.*, **23** (2024), 242. https://doi.org/10.1007/s12346-024-01081-1
14. S. Miao, Z. Y. Yin, Z. R. Li, C. Y. Pan, G. M. Wei, An analysis of the Lie symmetry and conservation law of a variable-coefficient generalized Calogero–Bogoyavlenskii–Schiff equation, *Mathematics*, **12** (2024), 3619. https://doi.org/10.3390/math12223619
15. B. Mohan, S. Kumar, Painlevé analysis, restricted bright-dark N-solitons and rogue waves for a (4+1)-dimensional generalized KP equation, *Nonlinear Dyn.*, **113** (2024), 11893–11906. https://doi.org/10.1007/s11071-024-10645-4

16. S. Shagolshem, B. Bira, K. V. Nagaraja, Analysis of soliton wave structure for coupled Higgs equation via Lie symmetry and unified method, *Nonlinear Dyn.*, **113** (2025), 11999–12020. https://doi.org/10.1007/s11071-024-10697-6

17. N. A. Kudryashov, Painlevé analysis of the Sasa–Satsuma equation, *Phys. Lett. A*, **525** (2024), 129900. https://doi.org/10.1016/j.physleta.2024.129900

18. S. Kumar, B. Mohan, A. Kumar, Generalized fifth-order nonlinear evolution equation for the Sawada-Kotera, Lax, and Caudrey-Dodd-Gibbon equations in plasma physics: Painlevé analysis and multi-soliton solutions, *Phys. Scr.*, **97** (2022), 035201. https://doi.org/10.1088/1402-4896/ac4f9d

19. A. M. Wazwaz, W. Alhejaili, S. A. El-Tantawy, On the Painlevé integrability and nonlinear structures to a (3+1)-dimensional Boussinesq-type equation in fluid mediums: Lumps and multiple soliton/shock solutions, *Phys. Fluids*, **36** (2024), 033116. https://doi.org/ 10.1063/5.0194071

20. S. Arshed, N. Raza, M. Kaplan, Painlevé analysis, dark and singular structures for pseudo-parabolic equations, *Mod. Phys. Lett. B*, **36** (2022), 2250104. https://doi.org/10.1142/S0217984922501044

21. J. G. Liu, Soliton structures for the (3+1)-dimensional Painlevé integrable equation in fluid mediums, *Sci. Rep.*, **14** (2024), 11581. https://doi.org/10.1038/s41598-024-62314-6

22. S. Kumar, B. Mohan, A generalized nonlinear fifth-order KdV-type equation with multiple soliton solutions: Painlevé analysis and Hirota Bilinear technique, *Phys. Scr.*, **97** (2022), 125214. https://doi.org/10.1088/1402-4896/aca2fa

23. S. Ahmad, S. Saifullah, A. Khan, M. Inc, New local and nonlocal soliton solutions of a nonlocal reverse space-time mKdV equation using improved Hirota bilinear method, *Phys. Lett. A*, **450** (2022), 128393. https://doi.org/10.1016/j.physleta.2022.128393

24. L. Yang, B. Gao, The nondegenerate solitons solutions for the generalized coupled higher-order nonlinear Schrödinger equations with variable coefficients via the Hirota bilinear method, *Chaos Soliton. Fract.*, **184** (2024), 115009. https://doi.org/10.1016/j.chaos.2024.115009

25. M. Raheel, A. Zafar, J. G. Liu, New periodic-wave, periodic-cross-kink wave, three wave and other analytical wave solitons of new (2+1)-dimensional KdV equation, *Eur. Phys. J. Plus*, **139** (2024), 50. https://doi.org/10.1140/epjp/s13360-023-04831-3

26. F. Yuan, B. Ghanbari, Interaction soliton solutions for the (2+1)-dimensional Hirota–Satsuma–Ito equation, *Nonlinear Dyn.*, **112** (2024), 2883–2891. https://doi.org/10.1007/s11071-023-09209-9

27. M. Raheel, A. Zafar, A. Bekir, K. U. Tariq, Interaction between kink solitary wave and rogue wave, new periodic cross-kink wave solutions and other exact solutions to the (4 + 1)-dimensional BLMP model, *J. Ocean Eng. Sci.*, (2022). https://doi.org/10.1016/j.joes.2022.05.020

28. U. K. Mandal, S. Malik, S. Kumar, A. Das, A generalized (2+1)-dimensional Hirota bilinear equation: integrability, solitons and invariant solutions, *Nonlinear Dyn.*, **111** (2023), 4593–4611. https://doi.org/10.1007/s11071-022-08036-8

29. S. Dutta, P. Chatterjee, K. K. Mondal, S. Nasipuri, G. Mandal, Solitons and resonance in fractional Sawada–Kotera equation using Hirota bilinear method, In: *Proceedings of the 2nd International Conference on Nonlinear Dynamics and Applications (ICNDA 2024)*, Cham: Springer, **405** (2024), 172–185. https://doi.org/10.1007/978-3-031-66874-6_14

30. S. Saifullah, S. Ahmad, M. A. Alyami, M. Inc, Analysis of interaction of lump solutions with kink-soliton solutions of the generalized perturbed KdV equation using Hirota-bilinear approach, *Phys. Lett. A*, **454** (2022), 128503. https://doi.org/10.1016/j.physleta.2022.128503

31. X. Lü, S. J. Chen, Interaction solutions to nonlinear PDEs via Hirota bilinear forms: one-lump-multi-stripe and one-lump-multi-soliton types, *Nonlinear Dyn.*, **103** (2021), 947–977. https://doi.org/10.1007/s11071-020-06068-6

32. W. Razzaq, A. Zafar, Machine learning-enhanced soliton solutions for the Lonngren-wave equation: An integration of Painlevé analysis and Hirota bilinear method, *Rend. Fis. Acc. Lincei*, **36** (2025), 917–932. https://doi.org/10.1007/s12210-025-01354-0

33. W. Razzaq, A. Zafar, Bilinearization of generalized Bogoyavlensky–Konopelchenko equation with neural networks: Painleve analysis, *Nonlinear Dyn.*, **113** (2025), 25083–25096. https://doi.org/10.1007/s11071-025-11384-w

AIMS Press